Title

Apoliprotein E-mediated ferroptosis controls cellular proliferation in chronic lymphocytic leukemia.

Journal

Leukemia, 39(1)

Authors

Nardi, Federica

Del Prete, Rosita

Drago, Roberta

et al.

Publication Date

2025

DOI

10.1038/s41375-024-02442-0

Peer reviewed

ARTICLE OPEN

Check for updates

CHRONIC LYMPHOCYTIC LEUKEMIA

Apoliprotein E-mediated ferroptosis controls cellular proliferation in chronic lymphocytic leukemia

Federica Nardi[1,2], Rosita Del Prete[1,13], Roberta Drago[1,3,13], Anthea Di Rita[1,4], Francesco Edoardo Vallone[5], Sara Ciofini[6], Margherita Malchiodi[6], Laura Pezzella[1], Laura Tinti[1], Vittoria Cicaloni[1], Laura Salvini[1], Danilo Licastro[7], Aidan T. Pezacki[8,9], Christopher J. Chang[8,9,10], Giuseppe Marotta[11], Antonella Naldini[12], Silvia Deaglio[5], Tiziana Vaisitti[5], Alessandro Gozzetti[6], Monica Bocchia[6] and Anna Kabanova[1]✉

Unraveling vulnerabilities in chronic lymphocytic leukemia (CLL) represents a key approach to understand molecular basis for its indolence and a path toward developing tailored therapeutic approaches. In this study, we found that CLL cells are particularly sensitive to the inhibitory action of abundant serum protein, apolipoprotein E (ApoE). Physiological concentrations of ApoE affect CLL cell viability and inhibit CD40-driven proliferation. Transcriptomics of ApoE-treated CLL cells revealed a signature of redox and metal disbalance which prompted us to explore the underlying mechanism of cell death. We discover, on one hand, that ApoE treatment of CLL cells induces lipid peroxidation and ferroptosis. On the other hand, we find that ApoE is a copper-binding protein and that intracellular copper regulates ApoE toxicity. ApoE regulation tends to be lost in aggressive CLL. CLL cells from patients with high leukocyte counts are less sensitive to ApoE inhibition, while resistance to ApoE is possible in transformed CLL cells from patients with Richter syndrome (RS). Nevertheless, both aggressive CLL and RS cells maintain sensitivity to drug-induced ferroptosis. Our findings suggest a natural suppression axis that mediates ferroptotic disruption of CLL cell proliferation, building up the rationale for choosing ferroptosis as a therapeutic target in CLL and RS.

Leukemia (2025) 39:122–133; https://doi.org/10.1038/s41375-024-02442-0

INTRODUCTION

High proportion of long-term non-progressors [1] in CLL might be indicative of efficient natural suppression mechanisms keeping the disease under control. Such mechanisms have been only marginally explored. They might be linked to intrinsic tumor vulnerabilities, studying which might shed light onto the complex biology of CLL and indicate new therapeutic targets with translational potential.

We previously described that CLL cells are characterized by an ectopic expression of the immunomodulatory cell surface receptor immunoglobulin-like transcript 3 (ILT3/LILRB4) [2]. Functional implications of its expression have not been fully elucidated. The selective presence of ILT3 on CLL B cells, but not healthy B cells, made us hypothesize that it might influence CLL biology in a considerable way. Previously, we found ILT3 to be a negative regulator of B cell receptor (BCR) signaling, selectively interfering with the Akt signaling axis [2]. Subsequently, a new physiological ligand for ILT3 has been identified as apolipoprotein E (ApoE) [3]. ApoE is an abundant serum protein regulating lipid transport between cells, tissues, and organs [4]. ApoE exists in three main isoforms (ApoE2, ApoE3, ApoE4), with ApoE3 being predominant and reaching 78% homozygosity in human population [5]. ApoE has been ascribed with anti-tumoral properties achieved via modulation of immunosuppressive myeloid cells [6, 7] and T lymphocytes [8]. It can also trigger intracellular signaling cascades [9].

Due to such versatility in the ApoE function, we set out to investigate whether it might be influencing the biology of CLL cells. We expressed lipoprotein-associated recombinant ApoE and used it for functional and biochemical investigation on primary CLL cell cultures mimicking the in vivo proliferative niche. ApoE was found to be toxic to proliferating CLL cells, hence we dissected the underlying mechanism and identified that ApoE induces ferroptosis, a type of cell death triggered by the accumulation of lipid peroxides which cause membrane damage and organelle disruption [10]. We also employed xenografts of primary tumor cells from patients with Richter syndrome (RS), to investigate whether resistance to ApoE-

[1]Fondazione Toscana Life Sciences, Siena, Italy. [2]Department of Medicine, Surgery and Neuroscience, University of Siena, Siena, Italy. [3]PhD program in Translational and Precision Medicine, University of Siena, Siena, Italy. [4]Department of Life Sciences, University of Siena, Siena, Italy. [5]Department of Medical Sciences, University of Turin, Turin, Italy. [6]Hematology, Department of Medicine, Surgery and Neurosciences, University of Siena, Siena, Italy. [7]AREA Science Park, Padriciano, Trieste, Italy. [8]Department of Chemistry, Princeton University, Princeton, NJ, USA. [9]Department of Chemistry, University of California, Berkeley, CA, USA. [10]Department of Molecular and Cell Biology, University of California, Berkeley, CA, USA. [11]Stem Cell Transplant and Cellular Therapy Unit, University Hospital of Siena, Siena, Italy. [12]Cellular and Molecular Physiology Unit, Department of Molecular and Developmental Medicine, University of Siena, Siena, Italy. [13]These authors contributed equally: Rosita Del Prete, Roberta Drago.
✉email: a.kabanova@toscanalifesciences.org

Received: 11 January 2024 Revised: 1 October 2024 Accepted: 14 October 2024
Published online: 23 October 2024

mediated suppression might arise in highly aggressive transformed CLL. Our findings suggest that ApoE targets CLL vulnerability to ferroptosis and that it is less pronounced in patients with aggressive CLL. Importantly, from translational perspective this vulnerability remains targetable by drugs, even when resistance to ApoE is acquired.

MATERIALS AND METHODS

Ethics approval and consent to participate

All methods were performed in accordance with the relevant guidelines and regulations. Research on human samples was approved by Comitato Etico Regionale per la Sperimentazione Clinica della Regione Toscana (study "TLS_LLC"). All human participants gave written informed consent. Research on animals was approved by the Italian Ministry of Health (authorization 578/2021-PR).

Isolation and culturing of B cells

Primary CLL cells and healthy memory B cells were isolated via immunoselection from peripheral blood of untreated CLL patients (Supplementary Table S1) and healthy donors, respectively. Xenografts of primary tumor cells from RS patients were derived as described [11, 12]. 25×10^3/well CLL cells were cultured in serum-free AIM-V medium (Thermo Scientific) in the presence of 25×10^3/well hCD40L-expressing irradiated 3T3 feeder cells, F(ab')2 Fragment Goat Anti-Human IgM Fc5µ (Jackson Immune Research), 25 ng/mL IL-21 and 10 ng/ml IL-4 (ImmunoTools; IL-4 was not used for RS cells). Cell viability and proliferation were evaluated upon 5-6 days of culture by flow cytometry using

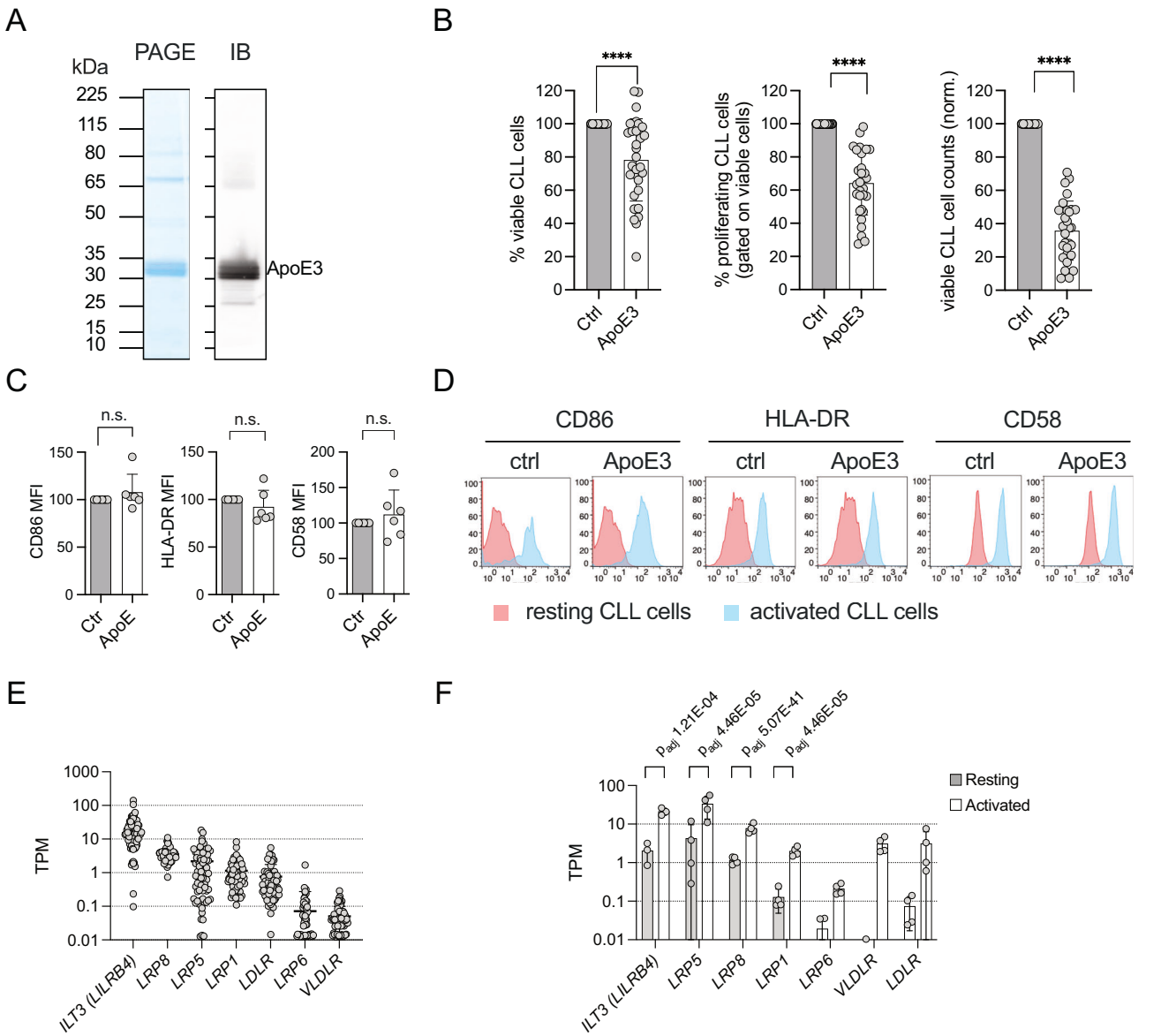

Fig. 1 CLL cells are sensitive to ApoE-mediated inhibition of cell proliferation. A SDS-PAGE and immunoblotting of recombinant ApoE3. **B** CLL cells activated in the presence of 3T3-CD40L feeder cells, α-IgM stimulatory antibodies and IL4/IL21 were treated with 50 µg/mL ApoE3 or control supernatant ($n = 29$ patients). Viability, proliferation of viable cells, and total counts of viable cells were assessed after 5 days of culturing. Values were normalized to controls treated with supernatants from Expi293 cells transfected with an empty vector. **C** Quantification and **D** representative flow cytometry profiles of CD86, HLA-DR, and CD58 on control and ApoE3-treated CLL cells 72 h post-activation ($n = 6$ donors). **E** RNAseq counts of ApoE receptors in blood-derived unstimulated CLL cells ($n = 78$ donors) from a published dataset [58]. **F** RNAseq counts of ApoE receptors in control and CD40L/α-IgM/IL4/IL21-activated CLL cells 96 h post-activation ($n = 4$ donors; study PRJNA973003). Graphs report mean values ± SD. $^*P < 0.05$, $^{***}P < 0.001$, $^{****}P < 0.0001$ (Mann-Whitney test); p adjusted are derived from DESeq2 results. TPM transcripts per million.

viability dye Zombie Aqua or Zombie Violet (BioLegend) and CFSE (ThermoFisher). Data analysis was carried out with FlowJo v9.0.

Reagents

We used Expi293-produced recombinant ApoE isoforms or control supernatants from mock-transfected cells (described in Supplementary materials); $ZnCl_2$ and $CuSO_4$ (Sigma Aldrich); copper activity-based probe CD649 [13]; Cu^{2+}-precomplexed elesclomol (BioVision and Selleck Chem); ferrostatin-1, deferoxamine, Z-VAD(OMe)-FKM, necrostatin-2 and ATN-224 (all Cayman Chemical); erastin-2 (Tocris Bioscence); ferric ammonium citrate (Sigma Aldrich). Immunoblotting and flow cytometry reagents are described in Supplementary materials.

Detection of lipid peroxidation and mitochondrial stress

50×10^3/well CLL cells, cultured as above, were treated with 50, 37, or 25 µg/mL ApoE or control supernatants. ApoE3-induced lipid peroxidation was evaluated by staining cells with 5 µM of the fluorescent fatty acid analog C11-BODIPY(581/591) (Life Technologies) [14]. Cells were imaged on the automated confocal system Opera Phenix (PerkinElmer) using 488/561 nm lasers and 500-550/570-630 nm emission filters. Image segmentation was performed to exclude cell debris/aggregates/feeder cells. Quantitative analysis was performed on Harmony software (PerkinElmer). Mitochondrial membrane potential and reactive oxygen species (ROS) were evaluated by flow cytometry by adding 100 nM MitoTracker Orange and 5 µM MitoSOX Red (ThermoFisher) to cells at 37 °C for 40 min and 25 min, respectively.

Bioinformatics analysis and RNAseq datasets used in this study

A detailed description of RNAseq analysis and public RNAseq datasets used in the study is provided in Supplementary Materials.

mRNA production and CLL B cell electroporation

The full-length cDNA of human SLC31A1 was amplified by reverse transcription of total RNA extracted from CLL B cells and subcloned into pRNA2-$(A)_{128}$ [15]. mRNA encoding for SLC31A1 and GFP were generated and used to electroporate 5×10^6 CFSE-stained CLL cells as previously described [16]. After electroporation 25×10^3/well B cells were plated in a 96 well plate pre-coated with 25×10^3/well hCD40L-3T3 feeder cells and IL-4/IL-21/antibody stimuli as described above. 25, 37, and 50 µg/ml ApoE3 were added on day 2 and cell viability and proliferation analyzed at day 6 post-electroporation. SLC31A1 over-expression was evaluated by immunoblotting 24 h after electroporation.

SDS-PAGE analysis of ApoE binding to copper probe CD649

2 µg of recombinant ApoE3 was resuspended in 50 µL PBS, in the presence or absence of 20 µM $CuSO_4$, for 5 min at RT. Then 2 µM CD649 probe was added for 2 h at RT. Samples were resuspended in SDS-PAGE loading buffer, boiled 5 min at 90 °C, and loaded in 4–12% polyacrylamide Bolt precast gels (ThermoFisher). Fluorescence (Ex/Em 633/670) was read on the ImageQuant LAS4000 biomolecular imager (GE Healthcare). Protein loading was checked by SimplyBlue SafeStain (Invitrogen).

Statistics

The exact sample size (*n*) for each experimental group/condition and statistical test is indicated in Figure legends. The sample size was set to include at least three primary samples. Similar sample size was used for comparisons, to ensure that variation within each group of data was similar. For every figure we applied the appropriate statistical test, including non-parametrical Mann-Whitney test *DESeq2* for RNAseq data performed as indicated in Supplementary Methods.

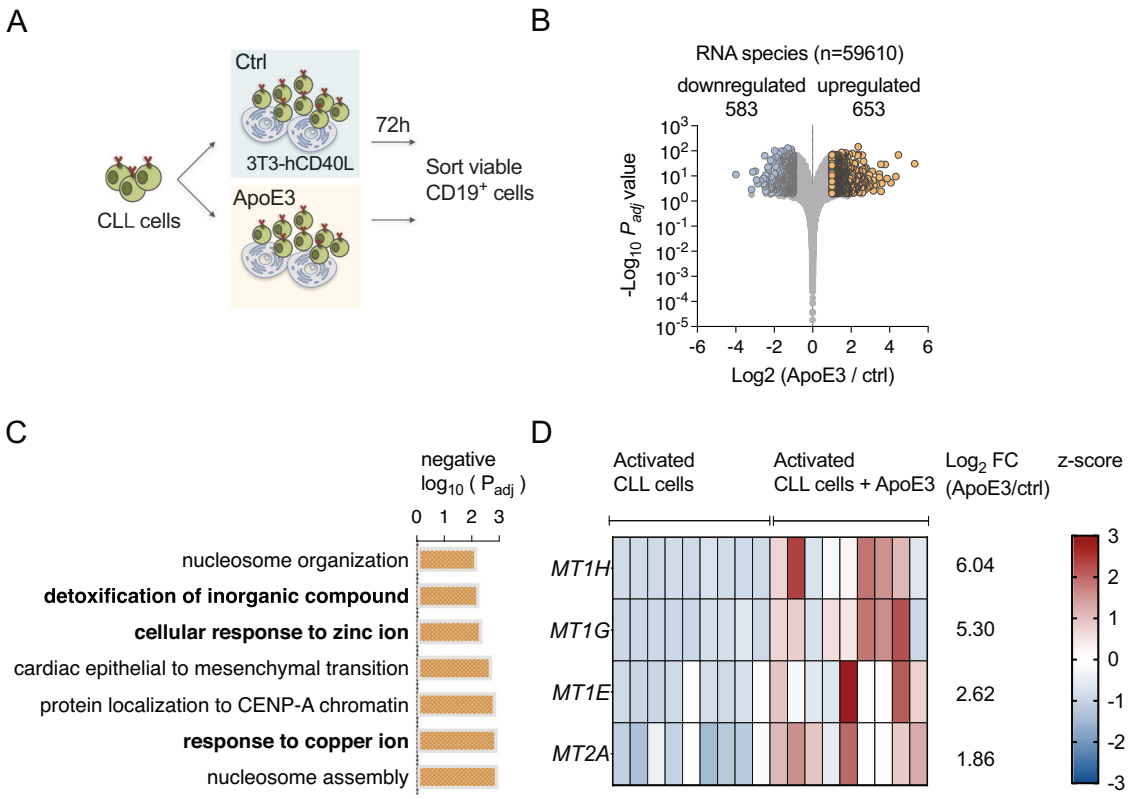

Fig. 2 ApoE suppression is linked to oxidative stress signature. A Schematic representation of RNAseq sample preparation (PRJNA769014 and PRJNA1135908). CLL cells were activated in co-cultures with 3T3-CD40L cells, α-IgM/IL-4/IL-21 cocktail, and 70 µg/ml recombinant ApoE3 or control supernatant for 72 h. Patients used for RNAseq analysis are indicated in Supplementary Table S1. **B** Volcano plot depicting RNAseq gene expression analysis on CLL cells treated with 70 µg/ml ApoE3 or control supernatant for 72 h as described in (**A**). Highlighted are significantly downregulated (blue) or upregulated (orange) RNA species. *P adjusted* and fold-change values were calculated by DESeq2. **C** Gene expression signatures upregulated following ApoE3 treatment as identified by gene enrichment analysis with gProfiler for Gene Onthology - Biological Process (log2 FC ≥ 1, $p_{adj} \leq 0.01$, Table 2S Tab 3). Redundant gene groups were filtered out. **D** Heatmap showing RNAseq counts of genes belonging to the "detoxification of Cu/Zn/Cd ions" group in (**C**). TPM transcripts per million.

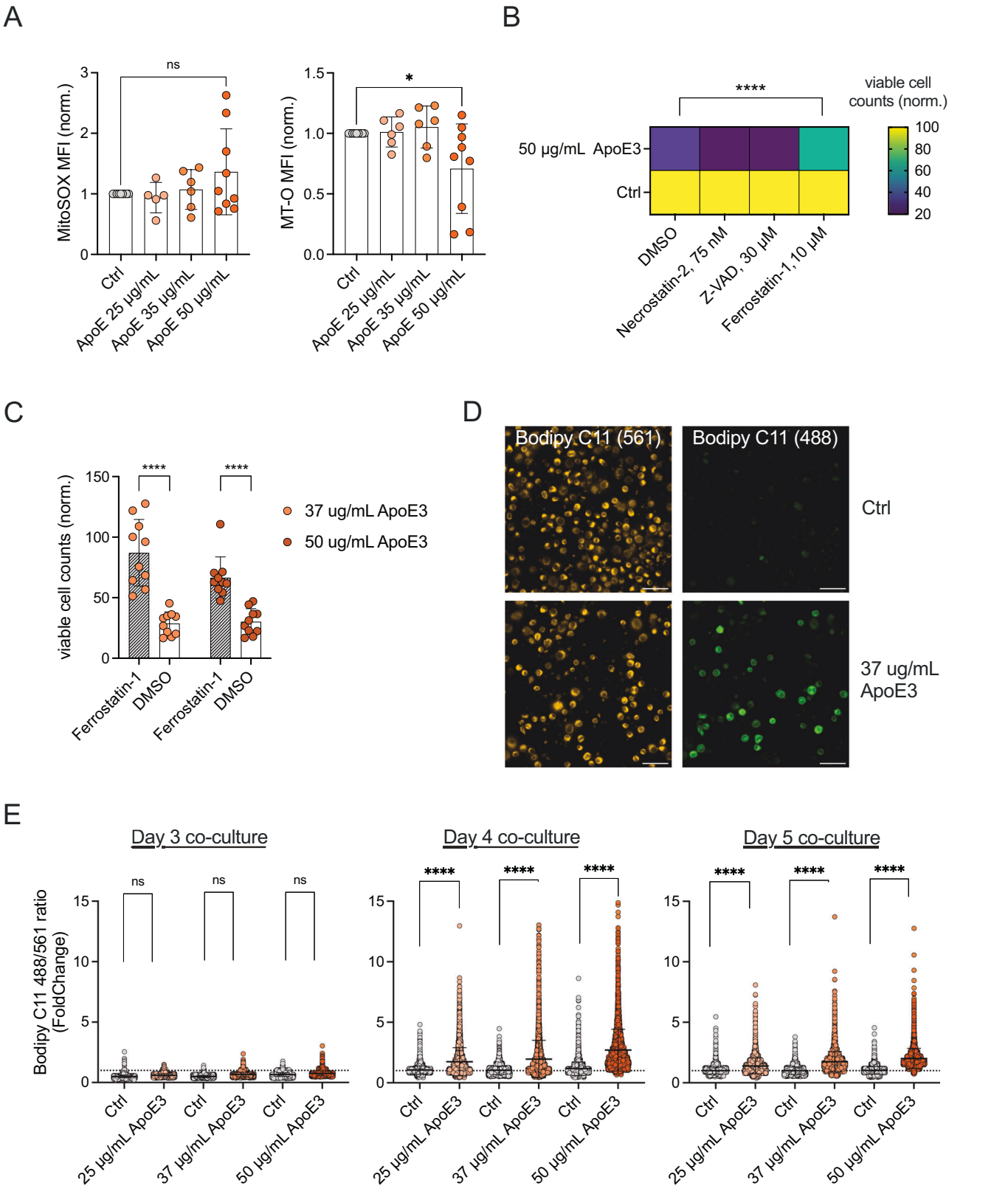

RESULTS

CLL cells are sensitive to ApoE-mediated inhibition of cell proliferation

We expressed recombinant ApoE isoforms in mammalian cells to produce concentrated lipoprotein-associated ApoE as described [9] (Fig. 1A and Supplementary Fig. S1). To evaluate ApoE influence on CLL cells, we used a co-culturing system that induces activation and proliferation of CLL cells via CD40/BCR engagement and IL-4/IL-21 stimulation, mimicking interactions in the CLL proliferative niche [17]. Incubation with ApoE3 affected CLL cell

Fig. 3 ApoE induces lipid peroxidation and ferroptosis in CLL cells. A CLL cells ($n = 5$–9 donors) were cultured with 3T3-CD40L cells, α-IgM/IL4/IL21 and indicated concentrations of ApoE or control supernatants for 4 days and stained with MitoSOX Red and MitoTracker orange (MT-O). Reported is mean florescence intensity (MFI) expressed as fold-change of ApoE-treated samples versus controls treated with supernatants from Expi293 cells transfected with an empty vector. **B** Heatmap showing viable CLL cell counts ($n = 6$–10 donors) stimulated for 5 days as in (**A**), in the presence of 50 µg/mL ApoE or control supernatants and indicated compounds. Values are normalized to the corresponding controls. **C** Viable cell counts of ApoE-treated CLL cell cultures ($n = 10$ donors) in the presence of 10 µM Ferrostatin-1 or DMSO. Values are normalized to the control group treated with control supernatants and DMSO. **D** Representative fluorescent images showing C11-BODIPY-stained CLL cells stimulated for 4 days as in (**A**) and treated with 50 µg/mL ApoE or control supernatants. **E** Time course analysis of BODIPY C11 oxidation in CLL cells ($n = 5$ donors) activated/treated for 3–5 days as in (**A**). For quantification, cells were filtered by size to exclude feeder cells and cell debris. Quantitative analysis was performed on 3000–5000 single cells per condition. The ratio of intensity of oxidized dye (488 nm excitation) vs reduced dye (561 nm excitation) was used as a readout of lipid peroxidation. Data are expressed as fold change normalized to the mean 488/561 ratio calculated on untreated samples. Graphs report mean values ± SD. $^{*}P < 0.05$, $^{****}P < 0.0001$ (Mann-Whitney test).

viability and proliferation, which resulted in a significant drop in viable cell numbers (Fig. 1B). No correlation was observed between ApoE ability to impair cell viability versus proliferation, suggesting that ApoE may exert a dual inhibitory role realized in the donor-dependent context. All three ApoE isoforms were efficient in inhibiting CLL proliferation at concentrations in the physiological range (IC50 18.3-49.8 µg/mL, Supplementary Fig. S2) [18]. Interestingly, ApoE inhibited proliferation of healthy memory B cells as well (Supplementary Fig. S3).

We observed that ApoE did not impact the early steps of CLL cell activation using as readout the upregulation of CD86, CD58, and HLA-DR (Fig. 1C, D). Instead, strong interference with the late stages of CLL cell activation (i.e., proliferation) let us hypothesize that receptors for ApoE might get upregulated following CLL cell stimulation. Analysis of RNAseq data from a published dataset of 78 patients allowed us to appreciate that, out of known ApoE receptors, ILT3 showed the highest levels expression in blood-derived unstimulated CLL cells (Fig. 1E). However, we observed that following CD40 engagement and cytokine stimulation, CLL cells upregulated the expression of several ApoE receptors (Fig. 1F), consistent with our prediction. Activation-induced upregulation of ApoE receptors was observed in healthy memory B cells as well (Supplementary Fig. S4).

ApoE treatment is associated with redox and metal disbalance signature in CLL cells

To get insight into the mechanism of ApoE-mediated inhibition, we compared gene expression profiles in activated CLL cells treated for 72 h with ApoE3 (the predominant genetic ApoE variant [5]) (Fig. 2A). Bioinformatics analysis of RNAseq data evidenced a considerable impact of ApoE3 on CLL cell transcriptomes (Fig. 2B, Supplementary Table S2) and modulated expression of genes belonging to various signaling pathways implicated in CLL pathogenesis (Supplementary Fig. S5). By analyzing genes significantly upregulated in ApoE3-treated cells, we observed a signature implicating several cellular pathways, including cellular response to metal toxicity (Fig. 2C). Specifically, transcriptomics evidenced upregulated expression of metallothioneins *M1E*, *MT1G*, *MT1H*, *MT2A* (Fig. 2D). These proteins scavenge ROS and bivalent metal ions, protecting cells from oxidative injury and heavy metal toxicity [19]. Hence, our data suggested a possible mechanism underlying ApoE-mediated cell death in CLL cells.

ApoE induces lipid peroxidation and ferroptosis in proliferating CLL cells

Firstly, we questioned whether CLL cells were suffering oxidative stress following ApoE3 treatment. ApoE has been previously implicated in the induction of mitochondrial ROS [20]. Measurement of mitochondrial ROS and mitochondrial potential in CLL cells revealed a trend indicative of mitochondrial oxidative stress in ApoE3-treated cells (Fig. 3A). To follow up on this observation, we performed cell death inhibitor screening using the apoptosis inhibitor Z-VAD, the necroptosis inhibitor necrostatin-2, and the ROS scavenger and ferroptosis inhibitor ferrostatin-1. Ferrostatin-1 was found to be the only inhibitor able to salvage CLL cells from ApoE-mediated toxicity (Fig. 3B), which we confirmed on the extended panel of donors (Fig. 3C).

Our data suggested that ApoE toxicity might be caused by ferroptosis, a regulated cell death program distinct from apoptosis and necroptosis. It is driven by lipid peroxidation [21] which metallothioneins are known to counteract [19]. To evaluate lipid peroxidation in ApoE-treated CLL cells we used the C11-BODIPY (581/592), a fatty acid analog that shifts fluorescence emission peak from 590 nm to 510 nm upon oxidation. Hence, lipid peroxidation could be assessed by calculating the ratio of reduced-vs-oxidized spectra emission. Using C11-BODIPY, we observed that ApoE3 induced lipid peroxidation in cultured CLL cells (Fig. 3D). Quantitative image analysis at the single cell level revealed that ApoE-mediated lipid damage started on day 4 of stimulation (Fig. 3E), when CLL cells typically start proliferating. This observation corroborated our hypothesis on the selective impact of ApoE upon late stages of CLL cell activation. Collectively, our findings suggested that ApoE toxicity against proliferating CLL cells is caused by ferroptosis that could be counteracted by ROS scavenging.

ApoE-induced ferroptosis occurs under hypoxic conditions and does not depend on iron supplementation

The partial pressure of oxygen (pO_2) in blood is close to 5%, while it could drop as low as 0.5-1% within the lymph node niche where CLL cells form proliferative centers [22]. Since O_2 is required for lipid peroxidation, we asked whether CLL cells cultured in hypoxia are still sensitive to ApoE toxicity. After setting up conditions for achieving CLL cell proliferation at 1% pO_2 (Supplementary Fig. S6A), we were able to appreciate the inhibitory effect of ApoE upon CLL cell proliferation (Supplementary Fig. S6B), as well as toxicity of the synthetic ferroptosis-inducer erastin-2 against them (Supplementary Fig. S6C). These data demonstrate that ApoE-mediated inhibition and ferroptosis in proliferating CLL cells can occur under hypoxic condition.

Iron is one of the main ferroptosis mediators catalyzing the production of free radicals that oxidize lipids [10]. We assessed whether iron overload might promote ferroptosis in CLL cells and whether iron availability could influence ApoE toxicity. Iron overloading using ferric ammonium citrate did not impact viability or proliferation of CLL cells (Supplementary Fig. S7A), whereas iron chelation with deferoxamine did not influence ApoE-mediated inhibition (Supplementary Fig. S7B). Hence, modulation of iron levels appears not to have a direct impact on ferroptosis or ApoE toxicity in proliferating CLL cells.

ApoE toxicity against CLL cells is regulated by copper

We explored a parallel hypothesis according to which ApoE inhibition might be associated with bivalent metal disbalance. Cell culture medium indeed contains two physiological bivalent metals, zinc (Zn^{2+}) and copper (Cu^{2+}), whose accumulation and associated toxicity are counteracted by the action of

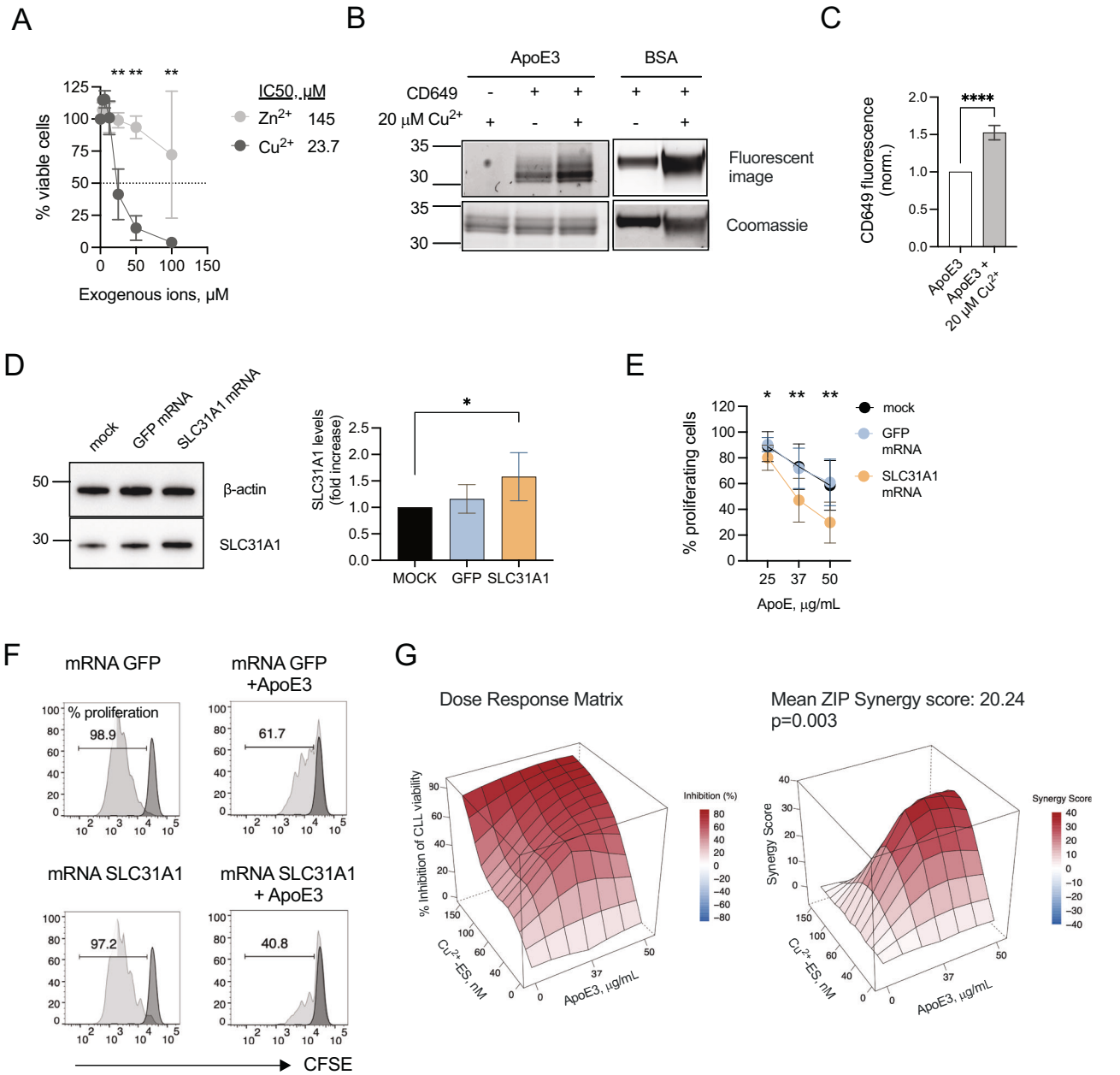

Fig. 4 ApoE is a copper-binding protein whose toxicity is regulated by intracellular copper levels. A Cell viability at different concentrations of $ZnCl_2$ and $CuSO_4$ was evaluated on CLL cells cultured with 3T3-CD40L cells and α-IgM/IL4/IL21 for 5–6 days ($n = 3$ donors). **B** Representative SDS-PAGE analysis of ApoE3 interaction with copper-selective probe CD649, as such or pre-incubated with 20 μM $CuSO_4$. Bovine serum albumin (BSA) was used as a copper-binding control. **C** Quantification of SDS-PAGE results ($n = 4$ independent experiments). **D** Immunoblotting (left panel) and its quantification (right panel) of SLC31A1 levels in CLL cells 24 h after electroporation with nothing (mock), *GFP* mRNA, or *SLC31A1* mRNA. **E** ApoE3-mediated inhibition of CLL cell proliferation after electroporation with nothing (mock), *GFP* mRNA or *SLC31A1* mRNA. **D**, **E** are representative of $n = 5$–7 independent experiments. **F** Representative flow cytometry analysis of CLL cell proliferation after electroporation and cultured with or without 37 μg/mL ApoE3. Histograms in dark gray depict non-proliferating cells. **G** Dose response matrix and ZIP synergy score of CLL cell viability upon their activation in the presence of ApoE3 and Cu^{2+}-precomplexed elesclomol. Synergy score was calculated in SynergyFinder package in *R* using the ZIP score model. CLL cells were cultured with 3T3-CD40L cells, cytokines, and indicated compounds for 6 days ($n = 8$ donors). Graphs report mean values ± SD. $^{*}P < 0.05$, $^{**}P < 0.01$; $^{****}P < 0.0001$ (Mann-Whitney test).

metallothioneins [23]. We established that CLL cells were relatively resistant to Zn^{2+} toxicity, while being sensitive to elevated concentrations of Cu^{2+} (Fig. 4A). It has been shown that ApoE is capable of binding Cu^{2+}-loaded resin [24]. To evaluate copper-binding properties of recombinant ApoE3, we used a chemical acyl imidazole probe CD649 that irreversibly binds to copper-binding proteins via bioconjugation [13]. CD649 was found to bind ApoE3 at basal conditions, with a significant increase when ApoE3 was pre-incubated with 20 μM Cu^{2+} (Fig. 4B, C and Supplementary Fig. S8), suggesting ApoE3 has a consistent capacity of copper binding.

To establish whether copper contributes to ApoE toxicity, we evaluated if sensitivity of CLL cells to ApoE could depend on intracellular copper concentrations. First, we assessed this by modulating levels of copper importers in CLL cells. By re-analyzing published proteomics results [25] we established that

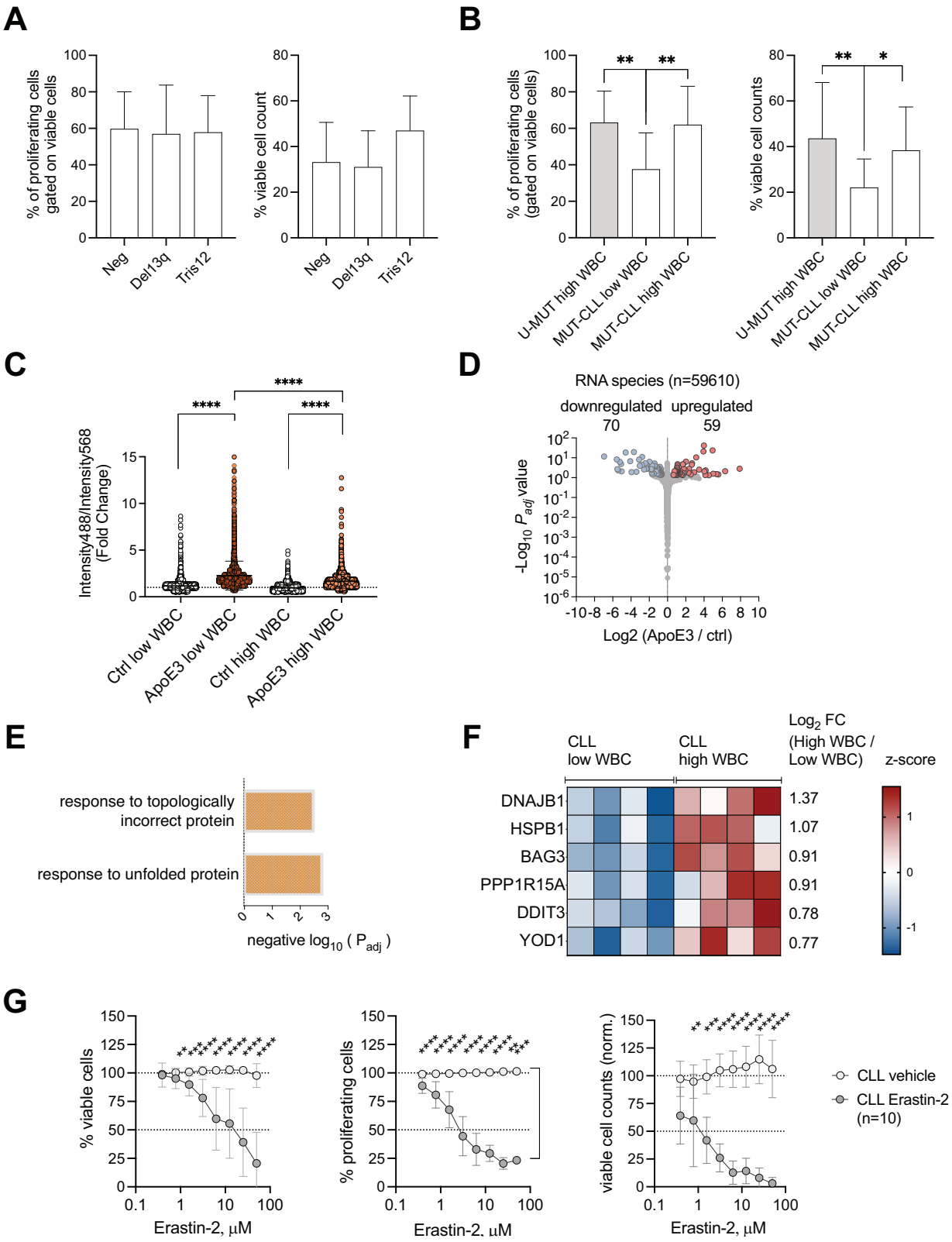

SLC31A1 is the only copper transporter expressed on the surface of CLL cells (Supplementary Fig. S9). We overexpressed SCL31A1 in CLL cells via mRNA electroporation [16] (Fig. 4D, E and Supplementary Fig. S10). This did not have an impact upon CLL cell proliferation on its own (Fig. 4F), however it raised CLL cell sensitivity to ApoE3 (Fig. 4E, F). Second, when Cu^{2+} was delivered into cells via a copper-selective ionophore elesclomol which bypasses cellular receptors [26, 27], a synergistic profile between ApoE and copper ions was observed (Fig. 4G). Hence, our data suggest that ApoE is a copper-binding protein and that

Fig. 5 Cells from CLL patients with high WBC display increased resistance to ApoE. A Percentage of viable proliferating cells and total counts of viable CLL cells from CLL patients without chromosomal aberrations (Neg, $n = 11$ donors), deletion of chromosome 13 (del13q, $n = 7$ donors), or trisomy 12 (tris12, $n = 3$ donors). CLL cells were grown with 3T3-CD40L cells, α-IgM/IL4/IL21, and treated with 50 μg/mL ApoE3 for 5–6 days. **B** Percentage of viable proliferating cells and total counts of viable CLL cells from patients with mutated (MUT) *IGHV* (low WBC $n = 7$ donors; high WBC $n = 9$ donors) and unmutated (U-MUT) *IGHV* (high WBC, $n = 10$ donors) cultured as in (**A**). Values in (**A**) and (**B**) are normalized to the control group treated with supernatants from Expi293 cells transfected with an empty vector. 20,000 WBC/μL was used as a threshold to define low and high WBC groups. Graphs report mean values ± SD. $^{*}P < 0.05$ and $^{**}P < 0.01$ (Mann-Whitney test). **C** Analysis of lipid peroxidation using BODIPY C11 comparing CLL cells from donors with low WBC ($n = 6$ donors) and high WBC ($n = 4$ donors). Controls were treated with supernatants from Expi293 cells transfected with an empty vector. Graph report mean values ± SD. **** $P < 0.0001$ (Mann-Whitney test). **D** Volcano plot depicting RNAseq gene expression analysis on CLL cells cultured for 72 h with 70 μg/ml ApoE3 or control supernatant. Highlighted are significantly downregulated (blue) or upregulated (orange) RNA species. *P adjusted* and fold-change values were calculated by DESeq2. Patients used for RNAseq analysis are indicated in Supplementary Table S1. **E** Gene expression signatures upregulated following ApoE3 treatment in cells from high WBC donors as identified by gene enrichment analysis with gProfiler for Gene Onthology—Biological Process (log2 FC ≥ 0.6, $p_{adj} \leq 0.05$, Table 3S Tab 3). **F** Heatmap showing RNAseq counts of genes belonging to the "response to unfolded protein" group in (**E**). **G** Viability (left panel), proliferation of viable cells (central panel) and total counts of viable cells (right panel) analyzed for CLL cells with high WBC ($n = 10$ donors) activated in co-cultures with 3T3-CD40L cells, α-IgM/IL-4/IL-21 cocktail and treated with various concentration of Erastin-2 or vehicle for 4–5 days. Values are normalized to the mean of the control group treated with vehicle (DMSO). Mann-Whitney test was performed for every single concentration point versus respective vehicle control. $^{**}P < 0.01$, $^{***}P < 0.001$, $^{****}P < 0.0001$.

its toxicity could be enhanced by increasing intracellular copper concentrations.

CLL aggressiveness associated with higher resistance to ApoE toxicity

CLL cells from different CLL donors showed heterogenous response to ApoE treatment (Fig. 1B). We, therefore, evaluated whether ApoE sensitivity could be influenced by genetic and clinical features of CLL. First, donors were stratified according to the presence of chromosomic aberrations (del13q, trisomy 12, neg) but no significant differences were observed (Fig. 5A). When donors were stratified according to the *IGHV* mutational status and white blood cell counts (WBCs), considering 20,000 WBC/μL as a threshold to define low or high WBC subgroups, we observed that CLL cells from low WBC donors were significantly more affected by ApoE treatment when considering *IGHV*-mutated (MUT) group (Fig. 5B). *IGHV* mutational status on its own did have effect when patients with similar WBC were compared (high WBC MUT donors vs high WBC U-MUT donors, Fig. 5B). We observed that increased resistance to ApoE toxicity in high WBC donors was associated with reduced lipid peroxidation (Fig. 5C). To get insight into the mechanisms underlying this phenotype, we performed RNAseq analysis which revealed a signature of unfolded proteins response (UPR) in ApoE-treated CLL cells from high WBC donors (Fig. 5D, E, Supplementary Table S4). Specifically, *DNAJB1*, *HSPB1*, *BAG3*, *PPP1R15A*, *DDIT3*, and *YOD1* genes were found to be upregulated (Fig. 5F). URP can counteract the endoplasmic reticulum stress by activating antioxidative machinery to restore homeostasis [28–30]. Moreover, *HSPB1* and *AEBP1* genes that were significantly upregulated in high WBC CLL (Fig. 5F and Supplementary Table S3, respectively) are known as negative regulators of ferroptosis [31, 32]. Interestingly, CLL cells from high WBC donors still retained sensitivity to the ferroptosis-inducing small drug erastin-2 (Fig. 5G). Altogether, these data suggest that CLL cells could activate transcriptional programs to counteract ApoE toxicity but are still sensitive to the pharmacological induction of ferroptosis.

Richter syndrome (RS) cells could become resistant to ApoE toxicity but not to ferroptosis

This data prompted us to assess ApoE sensitivity in transformed CLL B cells from Richter syndrome (RS) patients. RS is characterized by particularly poor survival and response to therapy [12]. Using RS patient-derived xenografts from three donors with different mutational profiles [11, 12] (Table S4), we optimized culturing conditions for RS cells allowing us to evaluate their viability and proliferation similarly to the CLL model (Figure S11). We observed that two RS cases, RS_IP867/17 and RS_1316, showed intrinsic resistance to ApoE inhibition (Fig. 6A, B). ApoE resistance was not associated with the loss of RS cell sensitivity to ferroptosis since erastin-2 was efficient in reducing viability of proliferating cells in RS cultures (Fig. 6C).

We further sought to evaluate whether ferroptosis resistance might be deduced from transcriptional profiles of RS cells. Comparative analysis of transcriptomes in 14 RS patients and 269 CLL patients revealed that, out of 21 genes previously implicated in conferring ferroptosis resistance [10, 21, 33], four (*CD44*, *GSS*, *GCLM*, *AKR1C3*) were found to be upregulated in RS cells (Fig. 6D). However, the statistical result for *CD44* was found to be influenced by outliers since the median of expression in RS cells (138.35 ± 868.64) versus CLL cells (147.00 ± 148.70) was comparable (Supplementary Table S5), and a separately conducted statistical comparison confirmed that *CD44* was not upregulated in RS cells (Supplementary Fig. S12). Meanwhile, glutathione synthetase (*GSS*), glutamate-cysteine ligase regulatory subunit (*GCLM*) and aldo-keto reductase family 1 member C3 (*AKR1C3)* were expressed at medium-low levels in RS cells, which probably explains the lack of protective effect of their expression against erastin-2-induced death (Fig. 6C). Notably, one of the major protectors against ferroptosis, glutathione peroxidase 4 (*GPX4*), was found to be significantly downregulated in RS cells (median TPM 39.29 ± 24.72 versus 107.76 ± 58.32; Fig. 6E). These data altogether suggested that, although RS cells seem to develop mechanisms of protection against ApoE-induced ferroptosis, they maintain sensitivity to drug-induced ferroptosis and do not display transcriptional signature indicative of ferroptosis resistance.

DISCUSSION

Our study describes a regulatory mechanism according to which an abundant serum protein ApoE inhibits the proliferation of CLL cells through ferroptotic cell death. The described mechanism might become compromised in aggressive CLL and particularly in transformed RS, where we detected cases of ApoE resistance. Nevertheless, both CLL cells and ApoE-resistant RS cells maintain sensitivity to drug-induced ferroptosis, suggesting a promising therapeutic target. Our results illustrate how a study of natural suppression mechanisms helps elucidate CLL vulnerabilities, adding to the emerging concept of ApoE-mediated tumor regulation [6–8] and consolidating the role of ferroptosis in controlling malignant B cells [34, 35].

The regulatory function of serum-derived proteins has been previously explored in the context of CLL. However, the focus has

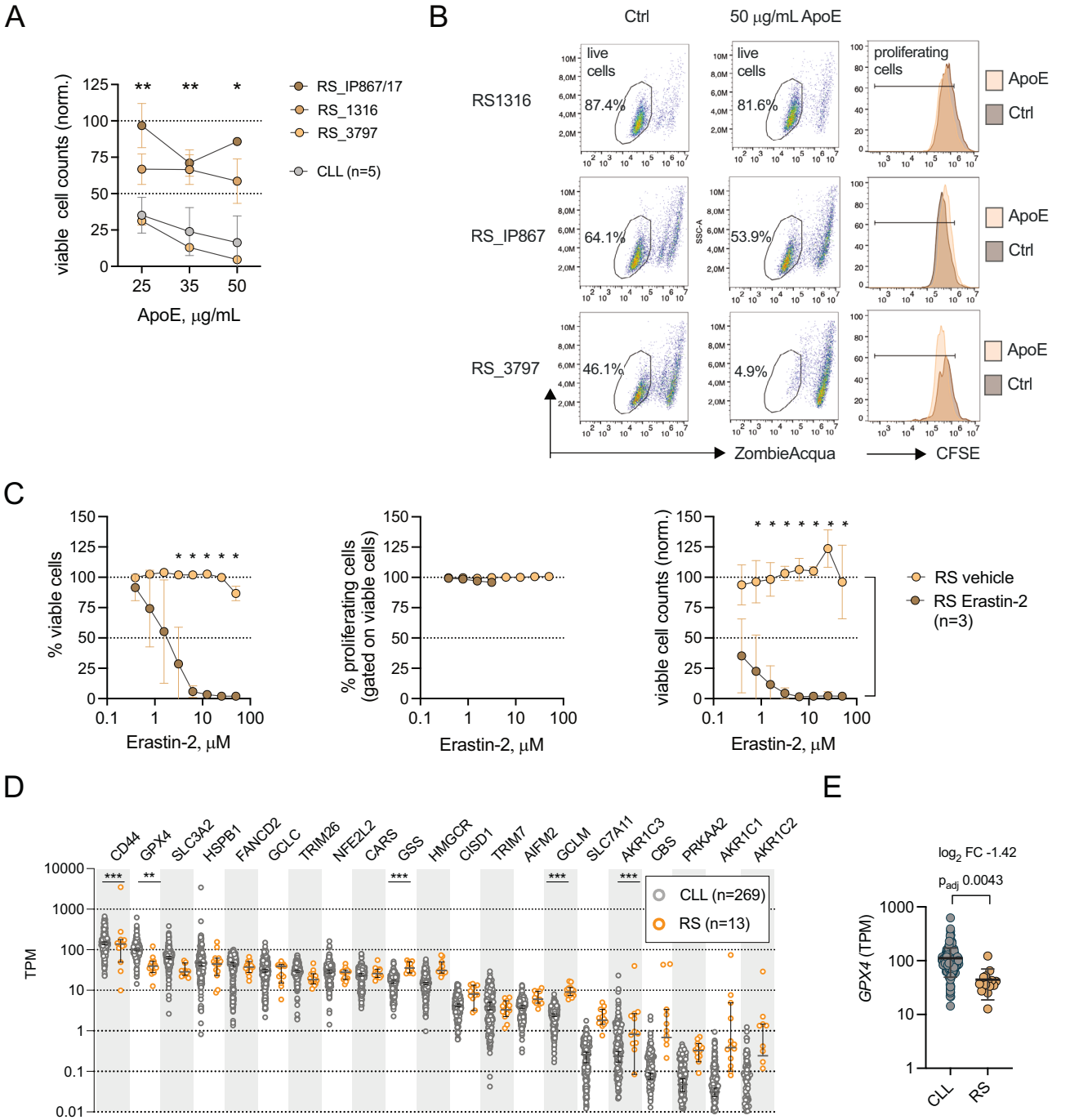

Fig. 6 RS cells could become resistant to ApoE toxicity but not to drug-induced ferroptosis. A Counts of viable CLL cells ($n = 5$ donors) and RS cells ($n = 3$ donors) from patient-derived xenografts cultured with 3T3-CD40L cells, α-IgM/IL21 and indicated concentrations of ApoE3 for 4-5 days. Values were normalized to controls treated with supernatants from Expi293 cells transfected with an empty vector. Statistical comparison was performed on RS_1316 and RS_IP867 samples versus CLL samples. Graphs report mean values ± SD. *$P < 0.05$, **$P < 0.01$ (Mann-Whitney test). **B** Representative flow cytometry profiles depicting cell viability and proliferation for three RS patient-derived xenografts cultured as above and treated with 50 μg/mL ApoE for 4 days. Percentages of proliferating RS cells are >70% in all conditions tested and are constant between Ctrl and ApoE conditions. **C** RS cells ($n = 3$ donors) were activated in the presence of 3T3-CD40L feeder cells, α-IgM stimulatory antibodies, and IL21, and treated with various concentrations of erastin-2. Viability (left panels), proliferation (central panels), and total counts of viable cells (right panels) were assessed after 4 days of culturing. Values are normalized to the mean of the control group treated with vehicle (DMSO). Mann-Whitney test was performed for every single concentration point versus respective vehicle control. Graphs report mean values ± SD. *$P < 0.05$. **D** RNAseq counts of ferroptosis resistance genes and (**E**) *GPX4* in a cohort of RS patients ($n = 14$) versus CLL cohort ($n = 269$ donors). TPM transcripts per million; *p adjusted* and fold-change expression values are derived from DESeq2 results.

fallen mostly on cytokines and immunomodulatory soluble proteins regulating inflammatory milieu [36] and antitumoral immune response [37, 38]. ApoE-mediated regulation of tumors is an emerging field. ApoE has been implicated in the modulation of anti-tumor immunity [6–8], however it has not been yet found to act upon tumor cells directly. ApoE ability to inhibit CLL proliferation suggests that it can counteract such strong signals as the BCR and CD40 triggering, which are considered to be driving forces sustaining CLL progression and resistance to therapy [39]. Exploring the biochemical basis of ApoE-mediated suppression revealed that it induces toxic lipid peroxidation. ApoE plays one of the central roles in orchestrating lipid homeostasis, as it normally coordinates cholesterol efflux from cells [4]. Whereas in pathogenic settings, such as Alzheimer's disease, the ApoE isoform ApoE4 promotes mitochondrial dysfunction [20] and pathogenic MAPK signaling [40]. In this context, our data outline a novel ApoE activity, as no previous evidence for ApoE ability to promote ferroptosis has been described.

Another interesting regulatory aspect of ApoE-mediated toxicity is that it could be potentiated by increasing intracellular copper concentrations, possibly due to the copper-binding properties of ApoE. Excess copper can induce production of ROS [41] that may exacerbate oxidative stress within cells, further potentiating cellular damage by ApoE. Moreover, copper has been recently shown to directly enhance ferroptosis in pancreatic cancer in vitro and in vivo by promoting degradation of GPX4. Our data hence reinforce the notion of synergy between intracellular copper and ferroptotic cell death and promote the concept of tumor cell regulation by copper.

The propensity of ApoE to inhibit cell proliferation points towards a possibility that it might exert most of its inhibitory action upon dividing CLL cells in the tumor niche, i.e., bone marrow and secondary lymphoid organs. ApoE could be delivered into CLL niches from blood. However, certain resident cells such as macrophages are considered to be major ApoE producers in tissues [4, 42]. Guided by single-cell RNAseq analysis of human bone marrow [43], we obtained preliminary data suggesting that mesenchymal stromal cells derived from CLL biopsy could secrete ApoE (Supplementary Fig. S13). Further exploiting the nature and targetability of ApoE-producing cells within the CLL microenvironment might become therapeutically relevant. Notably, a recent study comparing gene expression profiles of CLL cells from peripheral blood and lymph node biopsies identified *ApoE* among transcripts upregulated in lymph node samples from patients with clonally stable CLL [44]. Combined with our data, this might suggest that pharmacological upregulation of ApoE levels might counteract CLL progression and could be potentially enhanced by copper-delivery compounds, such as elesclomol [45] which we found to act in synergy with ApoE. A possible therapeutic approach to ApoE upregulation could be to use synthetic liver X receptor (LXR) agonizts that held great promise in various applications [46, 47] and have been reported to increase ApoE levels in vivo [48]. We, however, found that, in contrast to human mesenchymal stromal cells that appear to be responsive to LXR agonist GW3965 (Supplementary Fig. S13), splenocytes that constitute the primary CLL niche in the widely-used Eμ-TCL1 CLL model [49] are unable to upregulate ApoE secretion following GW3965 treatment, either in vitro or in vivo (Supplementary Fig. S14). Hence, there is a need to evaluate alternative compounds for the assessment of ApoE efficacy in preclinical models.

Finally, our data suggest that sensitivity to ApoE might be different across CLL spectrum, with decreased sensitivity in aggressive CLL and resistance arising during RS transformation. Our data associated URP signature with the increased resistance to ApoE toxicity suggesting that UPR might help ameliorating oxidative stress in ApoE-treated CLL cells due to its known antioxidative function [28–30, 32]. Interestingly, we find that CLL and RS cells are sensitive to drug-induced ferroptosis, even in cases of ApoE resistance. Several ferroptosis inducers have been showing promising effect in cancer therapy [10, 21]. In this context, our study suggests pharmacological induction of ferroptosis as a potential therapeutic approach in CLL and RS. It also improves our knowledge of molecular vulnerabilities in RS that have been yet poorly phenotypically characterized, although accounting for as much as 15% of total CLL cases [50]. Ferroptosis is a programmed cell death involving disbalance in redox homeostasis and lipid peroxidation, that has been recently proposed as a targetable vulnerability for many tumors, including diffuse large B-cell lymphoma [34, 35] and acute myeloid leukemia [51, 52]. CLL has been already characterized as highly prone to oxidative stress [53], which could act as a protective mechanism since indolent CLL is hypersensitive to redox disbalance [54]. Consequently, pharmacological induction of oxidative stress has been proposed as a therapeutic strategy in CLL [55, 56]. Overall, this strongly suggests that redox burden intrinsic to CLL cells might render them particularly sensitive to agents inducing ferroptosis. Moreover, induction of ferroptosis might represent a promising strategy to circumvent CLL resistance to apoptotic cell death and Bcl-2 inhibitors [57].

In conclusion, our findings illustrate that the exploration of natural suppressor mechanisms holds promise in revealing biochemical aspects of CLL regulation and therapeutic targets in CLL and RS.

DATA AVAILABILITY

All data generated during this study are included in Tables 2S and 3S; re-analyzed datasets are indicated in the "Public RNAseq datasets used" in Supplementary Materials. Raw RNAseq data generated in this study are available under accession numbers PRJNA973003, PRJNA769014, and PRJNA1135908.

REFERENCES

1. Kwok M, Oldreive C, Rawstron AC, Goel A, Papatzikas G, Jones RE, et al. Integrative analysis of spontaneous CLL regression highlights genetic and microenvironmental interdependency in CLL. Blood. 2020;135:411–28.
2. Zurli V, Wimmer G, Cattaneo F, Candi V, Cencini E, Gozzetti A, et al. Ectopic ILT3 controls BCR-dependent activation of Akt in B-cell chronic lymphocytic leukemia. Blood. 2017;130:2006–17.
3. Deng M, Gui X, Kim J, Xie L, Chen W, Li Z, et al. LILRB4 signalling in leukaemia cells mediates T cell suppression and tumour infiltration. Nature. 2018;562:605–9.
4. Mahley RW. Apolipoprotein E: cholesterol transport protein with expanding role in cell biology. Science. 1988;240:622–30.
5. Farrer LA, Cupples LA, Haines JL, Hyman B, Kukull WA, Mayeux R, et al. Effects of age, sex, and ethnicity on the association between apolipoprotein E genotype and Alzheimer disease: a meta-analysis. J Am Med Assoc. 1997;278:1349–56.
6. Tavazoie MF, Pollack I, Tanqueco R, Ostendorf BN, Reis BS, Gonsalves FC, et al. LXR/ApoE activation restricts innate immune suppression in cancer. Cell. 2018;172:825–.e18.
7. Bancaro N, Calì B, Troiani M, Elia AR, Arzola RA, Attanasio G, et al. Apolipoprotein E induces pathogenic senescent-like myeloid cells in prostate cancer. Cancer Cell. 2023;41:602–.e11.
8. Ostendorf BN, Bilanovic J, Adaku N, Tafreshian KN, Tavora B, Vaughan RD, et al. Common germline variants of the human APOE gene modulate melanoma progression and survival. Nat Med. 2020;26:1048–53.
9. Huang YWA, Zhou B, Wernig M, Südhof TC. ApoE2, ApoE3, and ApoE4 differentially stimulate APP transcription and Aβ secretion. Cell. 2017;168:427–441.e21.
10. Jiang X, Stockwell BR, Conrad M. Ferroptosis: mechanisms, biology and role in disease. Nat Rev Mol Cell Biol. 2021;22:266–82.
11. Vaisitti T, Braggio E, Allan JN, Arruga F, Serra S, Zamo A, et al. Novel Richter syndrome xenograft models to study genetic architecture, biology, and therapy responses. Cancer Res. 2018;78:3413–20.
12. Vaisitti T, Arruga F, Vitale N, Lee TT, Ko M, Chadburn A, et al. ROR1 targeting with the antibody-drug conjugate VLS-101 is effective in Richter syndrome patient-derived xenograft mouse models. Blood. 2021;137:3365–77.
13. Lee S, Chung CYS, Liu P, Craciun L, Nishikawa Y, Bruemmer KJ, et al. Activity-based sensing with a metal-directed acyl imidazole strategy reveals cell type-dependent pools of labile brain copper. J Am Chem Soc. 2020;142:14993–5003.

14. Murray MB, Leak LB, Lee WC, Dixon SJ. Protocol for detection of ferroptosis in cultured cells. STAR Protoc. 2023;4:102457.
15. Williams DJ, Puhl HL, Ikeda SR. A simple, highly efficient method for heterologous expression in mammalian primary neurons using cationic lipid-mediated mRNA transfection. Front Neurosci. 2010;4:1–20.
16. Nardi F, Pezzella L, Drago R, Di Rita A, Simoncelli M, Marotta G, et al. Assessing gene function in human B cells: CRISPR/Cas9-based gene editing and mRNA-based gene expression in healthy and tumor cells. Eur J Immunol. 2022;52:1362–5.
17. Schleiss C, Ilias W, Tahar O, Güler Y, Miguet L, Mayeur-Rousse C, et al. BCR-associated factors driving chronic lymphocytic leukemia cells proliferation ex vivo. Sci Rep. 2019;9:1–12.
18. Uchida Y, Ito S, Nukina N. Sandwich ELISA for the measurement of Apo-E4 levels in serum and the estimation of the allelic status of Apo-E4 isoforms. J Clin Lab Anal. 2000;14:260–4.
19. Thomas JP, Bachowski GJ, Girotti AW. Inhibition of cell membrane lipid peroxidation by cadmium- and zinc-metallothioneins. Biochim Biophys Acta. 1986;884:448–61.
20. Orr AL, Kim C, Jimenez-Morales D, Newton BW, Johnson JR, Krogan NJ, et al. Neuronal apolipoprotein E4 expression results in proteome-wide alterations and compromises bioenergetic capacity by disrupting mitochondrial function. J Alzheimer's Dis. 2019;68:991–1011.
21. Stockwell BR, Friedmann Angeli JP, Bayir H, Bush AI, Conrad M, Dixon SJ, et al. Ferroptosis: a regulated cell death nexus linking metabolism, redox biology, and disease. Cell. 2017;171:273–85.
22. Koers J, Marsman C, Steuten J, Tol S, Derksen NIL, ten Brinke A, et al. Oxygen level is a critical regulator of human B cell differentiation and IgG class switch recombination. Front. Immunol. 2022;13:1082154. https://doi.org/10.3389/fimmu.2022.1082154.
23. Cobine PA, Moore SA, Leary SC. Getting out what you put in: copper in mitochondria and its impacts on human disease. Biochim Biophys Acta—Mol Cell Res. 2021;1868:118867.
24. Miyata M, Smith JD. Apolipoprotein E allele-specific antioxidant activity and effects on cytotoxicity by oxidative insults and β-amyloid peptides. Nat Genet. 1996;14:55–61.
25. Zurli V, Montecchi T, Heilig R, Poschke I, Volkmar M, Wimmer G, et al. Phosphoproteomics of CD2 signaling reveals AMPK-dependent regulation of lytic granule polarization in cytotoxic T cells. Sci Signal. 2020;13. https://doi.org/10.1126/scisignal.aaz1965.
26. Tsvetkov P, Detappe A, Cai K, Keys HR, Brune Z, Ying W, et al. Mitochondrial metabolism promotes adaptation to proteotoxic stress. Nat Chem Biol. 2019;15:681–9.
27. Krasnovskaya O, Naumov A, Guk D, Gorelkin P, Erofeev A, Beloglazkina E, et al. Copper coordination compounds as biologically active agents. Int J Mol Sci. 2020;21. https://doi.org/10.3390/ijms21113965.
28. Ong G, Logue SE. Unfolding the interactions between endoplasmic reticulum stress and oxidative stress. Antioxidants. 2023;12. https://doi.org/10.3390/antiox12050981.
29. Zhang Z, Zhang L, Zhou L, Lei Y, Zhang Y, Huang C. Redox signaling and unfolded protein response coordinate cell fate decisions under ER stress. Redox Biol. 2019;25:101047.
30. Shimizu Y, Hendershot LM. Oxidative folding: cellular strategies for dealing with the resultant equimolar production of reactive oxygen species. Antioxid Redox Signal. 2009;11:2317–31.
31. Zhou Q, Wang X, Zhang Y, Wang L, Chen Z. Inhibition of AEBP1 predisposes cisplatin-resistant oral cancer cells to ferroptosis. BMC Oral Health. 2022;22:478.
32. Sun X, Ou Z, Xie M, Kang R, Fan Y, Niu X, et al. HSPB1 as a novel regulator of ferroptotic cancer cell death. Oncogene. 2015;34:5617–25.
33. Tang D, Chen X, Kang R, Kroemer G. Ferroptosis: molecular mechanisms and health implications. Cell Res. 2021;31:107–25.
34. Cai Y, Lv L, Lu T, Ding M, Yu Z, Chen X, et al. α-KG inhibits tumor growth of diffuse large B-cell lymphoma by inducing ROS and TP53-mediated ferroptosis. Cell Death Discov. 2023;9:182.
35. Schmitt A, Xu W, Bucher P, Grimm M, Konantz M, Horn H, et al. Dimethyl fumarate induces ferroptosis and impairs NF-κB/STAT3 signaling in DLBCL. Blood. 2021;138:871–84.
36. Yan XJ, Dozmorov I, Li W, Yancopoulos S, Sison C, Centola M, et al. Identification of outcome-correlated cytokine clusters in chronic lymphocytic leukemia. Blood. 2011;118:5201–10.
37. Nückel H, Switala M, Sellmann L, Horn PA, Dürig J, Dührsen U, et al. The prognostic significance of soluble NKG2D ligands in B-cell chronic lymphocytic leukemia. Leukemia. 2010;24:1152–9.
38. Landeira-Viñuela A, Arias-Hidalgo C, Juanes-Velasco P, Alcoceba M, Navarro-Bailón A, Pedreira CE, et al. Unravelling soluble immune checkpoints in chronic lymphocytic leukemia: physiological immunomodulators or immune dysfunction. Front Immunol. 2022;13:1–18.
39. Ondrisova L, Mraz M. Genetic and non-genetic mechanisms of resistance to BCR signaling inhibitors in B cell malignancies. Front Oncol. 2020;10:1–16.
40. Huang YWA, Zhou B, Nabet AM, Wernig M.Südhof TC. Differential signaling mediated by ApoE2, ApoE3, and ApoE4 in human neurons parallels Alzheimer's disease risk. J Neurosci. 2019;39:7408–27.
41. Xue Q, Kang R, Klionsky DJ, Tang D, Liu J, Chen X. Copper metabolism in cell death and autophagy. Autophagy. 2023;19:2175–95.
42. Liu L, MacKenzie KR, Putluri N, Maletić-Savatić M, Bellen HJ. The glia-neuron lactate shuttle and elevated ROS promote lipid synthesis in neurons and lipid droplet accumulation in glia via APOE/D. Cell Metab. 2017;26:719–737.e6.
43. Hay SB, Ferchen K, Chetal K, Grimes HL, Salomonis N. The Human Cell Atlas bone marrow single-cell interactive web portal. Exp Hematol. 2018;68:51–61.
44. Sun C, Chen Y-C, Martinez AZ, Baptista MJ, Pittaluga S, Liu D, et al. The immune microenvironment shapes transcriptional and genetic heterogeneity in chronic lymphocytic leukemia. Blood Adv. 2022. https://doi.org/10.1182/bloodadvances.2021006941.
45. Guthrie LM, Soma S, Yuan S, Silva A, Zulkifli M, Snavely TC, et al. Elesclomol alleviates Menkes pathology and mortality by escorting Cu to cuproenzymes in mice. Science. 2020;368:620–5.
46. Buñay J, Fouache A, Trousson A, de Joussineau C, Bouchareb E, Zhu Z, et al. Screening for liver X receptor modulators: where are we and for what use? Br J Pharm. 2021;178:3277–93.
47. Brendolan A, Russo V. Targeting cholesterol homeostasis in hematopoietic malignancies. Blood. 2022;139:165–76.
48. Fan J, Qi Zhao R, Parro C, Zhao W, Chou HY, Robert J, et al. Small molecule inducers of ABCA1 and apoE that act through indirect activation of the LXR pathway. J Lipid Res. 2018;59:830–42.
49. Bichi R, Shinton SA, Martin ES, Koval A, Calin GA, Cesari R, et al. Human chronic lymphocytic leukemia modeled in mouse by targeted TCL1 expression. Proc Natl Acad Sci. 2002. https://doi.org/10.1073/pnas.102181599.
50. Parry EM, Ten Hacken E, Wu CJ. Richter syndrome: novel insights into the biology of transformation. Blood. 2023;142:11–22.
51. Grignano E, Cantero-Aguilar L, Tuerdi Z, Chabane T, Vazquez R, Johnson N, et al. Dihydroartemisinin-induced ferroptosis in acute myeloid leukemia: links to iron metabolism and metallothionein. Cell Death Discov. 2023;9:97.
52. Akiyama H, Zhao R, Ostermann LB, Li Z, Tcheng M, Yazdani SJ, et al. Mitochondrial regulation of GPX4 inhibition-mediated ferroptosis in acute myeloid leukemia. Leukemia. 2023. https://doi.org/10.1038/s41375-023-02117-2.
53. Jitschin R, Hofmann AD, Bruns H, Giessl A, Bricks J, Berger J, et al. Mitochondrial metabolism contributes to oxidative stress and reveals therapeutic targets in chronic lymphocytic leukemia. Blood. 2014;123:2663–72.
54. Cavallini C, Chignola R, Dando I, Perbellini O, Mimiola E, Lovato O, et al. Low catalase expression confers redox hypersensitivity and identifies an indolent clinical behavior in CLL. Blood. 2018;131:1942–54.
55. Graczyk-Jarzynka A, Goral A, Muchowicz A, Zagozdzon R, Winiarska M, Bajor M, et al. Inhibition of thioredoxin-dependent H_2O_2 removal sensitizes malignant B-cells to pharmacological ascorbate. Redox Biol. 2019;21:101062.
56. Yosifov DY, Idler I, Bhattacharya N, Reichenzeller M, Close V, Ezerina D, et al. Oxidative stress as candidate therapeutic target to overcome microenvironmental protection of CLL. Leukemia. 2020;34:115–27.
57. Thus YJ, Eldering E, Kater AP, Spaargaren M. Tipping the balance: toward rational combination therapies to overcome venetoclax resistance in mantle cell lymphoma. Leukemia. 2022;36:2165–76.
58. Beekman R, Chapaprieta V, Russiñol N, Vilarrasa-Blasi R, Verdaguer-Dot N, Martens JHA, et al. The reference epigenome and regulatory chromatin landscape of chronic lymphocytic leukemia. Nat Med. 2018;24:868–80.

ACKNOWLEDGEMENTS

We would like to thank Simona Tavarini (GSK Vaccines, Siena, Italy) for technical help with cell sorting and Dr. Yu-Wei Alvin Huang (Brown University, US) for constructs for recombinant ApoE production. We would like to thank Prof. Andrea Brendolan and Vincenzo Russo (San Raffaele Hospital, Milan, Italy) for reagents and technical tips on LXR agonist use in vivo. We thank Dr. Malgorzata Firczuk and Lukasz Komorowski (Medical University of Warsaw, Poland) for their advice on synergy data analysis. This work was carried out with the support of Italian Association for Cancer Research (AIRC), grant MFAG-21495 to AK; AIRC postdoctoral fellowship Michele e Carlo Ardizzone 26636-2021 to RDP; support from Fondazione Toscana Life Sciences and the European Union - NextGenerationEU through the Italian Ministry of University and Research under PNRR - M4C2-I1.3 Project PE_00000019 "HEAL ITALIA" CUP B63D22000680006. The views and opinions expressed are those of the authors only and do not necessarily reflect those of the European Union or the European Commission. Neither the European Union nor the European Commission can be held responsible for them. CJC thanks the NIH (GM 79465) for support and is a CIFAR Fellow. TV thanks the AIRC MFAG-23107 for support.

AUTHOR CONTRIBUTIONS

FN, RDP, RD, ADR, and LP performed research and analyzed data. FN and AK wrote the manuscript. FEV performed bioinformatics analysis of RNAseq data on RS samples. LT, VC, and LS produced and characterized recombinant ApoE. DL performed and analyzed RNAseq data. SC, MM, GM, AG, and MB provided clinical material. ATP and CJC provided copper imaging reagents, advised on experimental design, and analyzed data. SD and TV provided RS patient-derived xenograft cells and RNAseq data on RS samples. AN provided equipment for experiments in hypoxia and advised on experimental design. AK directed the study and raised funding.

COMPETING INTERESTS

The authors declare no competing interests.

ADDITIONAL INFORMATION

Supplementary information The online version contains supplementary material available at https://doi.org/10.1038/s41375-024-02442-0.

Correspondence and requests for materials should be addressed to Anna Kabanova.

Reprints and permission information is available at http://www.nature.com/reprints

Publisher's note Springer Nature remains neutral with regard to jurisdictional claims in published maps and institutional affiliations.